Journal of The Electrochemical Society, **154** (12) A1112-A1117 (2007)
0013-4651/2007/154(12)/A1112/6/$20.00 © The Electrochemical Society

Solid-State NMR and Electrochemical Dilatometry Study on Li^+ Uptake/Extraction Mechanism in SiO Electrode

Taeahn Kim, Sangjin Park, and Seung M. Oh*,z

School of Chemical and Biological Engineering and Research Center for Energy Conversion and Storage, Seoul National University, Seoul 151-744, South Korea

This work reports the Li^+ uptake/extraction mechanism in silicon monoxide (SiO) as the negative electrode in lithium secondary batteries. A combined study of solid-state ^{29}Si- and ^{7}Li-nuclear magnetic resonance (NMR), electrochemical dilatometry, and charge-discharge cycling consistently demonstrates that the SiO_2 domain in SiO irreversibly reacts with Li^+ to produce lithium silicates and Li_2O in the first discharging period, whereas the elemental Si domain reversibly reacts, delivering the same charge-discharge characteristics to those of conventional amorphous Si electrodes. The volume expansion accompanied by the irreversible reaction is less significant than that caused by the lithiation of Si domain. The postmortem analysis made on cycled electrodes reveals a phase segregation between the lithium silicates/Li_2O and lithiated Si phase. It is likely that the lithium silicates/Li_2O phase plays a buffering role against the volume change of Si matrix, but the crack formation at the phase boundaries and eventual pulverization are still a problem to be solved.
 [DOI: 10.1149/1.2790282]

Manuscript submitted February 28, 2007; revised manuscript received August 29, 2007. Available electronically October 15, 2007.

Recently, many efforts have been made to replace the carbon-based anode with Li-alloy materials such as Si and Sn. Even if Si is known to have a higher theoretical capacity ($Li_{15}Si_4$: 3579 mAh g^{-1}) than that of graphite, it has not been used as an anode in a practical battery mainly due to a severe volume change encountered with cycling.[1-3] To overcome or alleviate this problem, several approaches have been made with nanosized Si powders,[4,5] active/inactive composites (for instance, Si/TiN, Si/TiB_2, and Si/FeSi),[6-8] and Si/carbon composites.[9,10] Rather surprisingly, however, the literature dealing with silicon monoxide (SiO) as the negative electrode for lithium cells is still limited even if this chemical is commercially available with a reasonable price.[11-14] This may be because the diffraction methods commonly used to solve structures of crystalline materials cannot provide useful structural data for these amorphous systems. The microscopic structure of SiO is still controversial. Two models have been proposed in the literature, the random-bonding (RB) and random-mixture (RM) models.[15-18] The former describes SiO as a single-phase material, wherein Si–Si and Si–O bonds are supposed to be randomly distributed throughout a continuous network.[15] The latter model, however, describes SiO as a mixture of amorphous elemental Si and SiO_2 domains of <10 Å in size.[16] Even if the literature dealing with the electrochemical behavior of SiO did not provide a clear structural description on SiO, some informative results concerning the reaction products formed after cycling have been presented.[11-14] For instance, Miyachi et al. have reported the generation of phase mixture, nanosized Si and lithium silicates, after an electrochemical charge-discharge cycling on SiO thin-film electrode.[19] The formation of elemental Si and lithium silicates by a nonelectrochemical pathway, a high-energy ballmilling with metallic lithium, was also evidenced by Yang and co-workers.[20]

This work has been motivated by a premise that SiO might be a better choice than its nonoxide counterpart when the issue of volume change is solely considered. That is, the absolute volume expansion of SiO should be smaller than that of Si because the absolute amount of Si in SiO is lower than in pure Si. Moreover, any oxygen-containing materials, SiO_2 and/or lithium silicates that are known to be generated during cycling, can play a buffering role against the volume change of Si domain. Another favorable feature expected with SiO is that the nanosized Si and SiO_2 domain, if the RM model is the right one, may give an unusual electrochemical reactivity that cannot be obtained with bulkier materials. In fact, unexpected electrochemical behaviors have been observed in many nanosized single- or mixed-phase materials: alloys,[21] metal oxides,[22-24] and metal halides.[25,26]

After reviewing the problems encountered with SiO electrode and the expectations projected above, the following goals have been identified in this work: (*i*) identification of a more realistic model for the microstructure of SiO, (*ii*) the Li^+ uptake/extraction mechanism, and the nature of reaction products and their effects on the anodic performance of SiO electrode, (*iii*) the extent of volume change in SiO electrode upon Li^+ uptake/extraction, and (*iv*) any unexpected reactivity associated with nanosized crystalline and/or amorphous mixture. The galvanostatic charge-discharge cycling was carried out to examine the anodic performance of SiO electrode, whereas any volume change evolved during cycling was traced with electrochemical dilatometry. The reaction products were analyzed by solid-state ^{7}Li and ^{29}Si nuclear magnetic resonance (NMR) technique, and morphological change was examined with a transmission electron microscope (TEM).

Experimental

The used SiO powder (325 mesh) was purchased from Aldrich Chemical Company and used as received. To prepare the negative electrodes, a mixture of SiO, Super P (as a carbon additive for conductivity enhancement), and polyvinylidene fluoride (PVdF, as a polymeric binder) in 80:10:10 weight ratio was dispersed in *N*-methyl pyrrolidone (NMP) and homogenized. The resulting slurry was spread on a piece of copper foil (10 μm thickness and 1 cm^2 apparent area) and dried in vacuum at 120°C for 12 h. It was then pressed to enhance the interparticle contact and to ensure a better adhesion to the current collector. For the electrochemical dilatometry experiment, however, the electrode composition was changed to 75:5:25 in weight ratio because a larger amount of polymeric binder (PVdF) was needed to minimize the electrode deformation. A beaker-type three-electrode cell was employed to assess the electrochemical performance of the samples. Lithium foils (Cyprus Co.) were used as the counter and reference electrode, and 1.0 M $LiClO_4$ dissolved in a mixture of ethylene carbonate (EC) and diethyl carbonate (DEC) (1:1, v/v) was used as the electrolyte. Galvanostatic charge-discharge cycling was made at a current density of 100 mA g^{-1} in the voltage range of 0.0–2.0 V (vs Li/Li^+) with a battery-testing system (Toyo Co.). The electrode swelling and contraction was monitored using a homemade electrochemical dilatometer.[27,28] For the solid-state NMR study, the cycled cells were disassembled in an argon-filled dry box and the electrode materials were scraped from the current collector and washed with dimethyl carbonate. The magic-angle-spinning (MAS)-NMR spectra were recorded with a Bruker DSX-400 NMR spectrometer. The ^{7}Li

* Electrochemical Society Active Member.
z E-mail: seungoh@snu.ac.kr

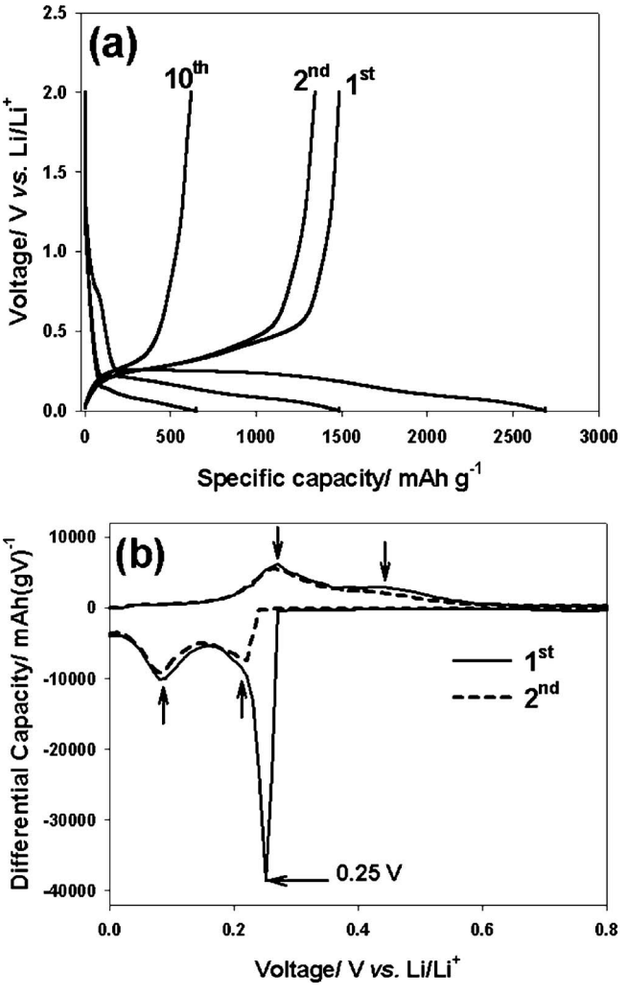

Figure 1. (a) The galvanostatic discharge-charge voltage profiles traced with SiO electrode and (b) the differential-capacity plots (dQ/dV vs V) for the initial two cycles.

spectra were obtained at a Larmor frequency of 155.5 MHz with 1.3 μs pulses and 0.2 s recycle delays and the ^{29}Si spectra at 79.5 MHz with 2.0 μs pulses and 10.0 s recycle delays. The ^{7}Li and ^{29}Si chemical shifts were referenced to 1.0 M LiCl and tetramethysilane (TMS), respectively. For referencing purposes, Li_4SiO_4 powder was prepared by firing a mixture of SiO (Aldrich Chemical Company) and LiOH (Aldrich Chemical Company, 99%) at 800°C for 10 h in a tubular furnace under air flow. The microscopic investigation was carried out with a JEOL JEM 2000 EXII TEM. In this work, the Li^+ uptake was expressed as discharging and the extraction as charging.

Results and Discussion

Typical galvanostatic discharge-charge voltage profiles observed with the SiO electrode are reproduced in Fig. 1a, where the lower profiles correspond to the discharging (lithiation) curves and the upper ones to the charging (delithiation) curves. In the first cycle, the specific discharge and charge capacity was 2680 and 1470 mAh g^{-1}, respectively, reflecting a large amount of irreversible capacity (1210 mAh g^{-1}) being generated. The much-reduced or negligible irreversible capacity from the second cycle reflects that the irreversible reaction takes place mainly in the first cycle. The plateau appeared at 0.8 V (vs Li/Li^+), which is likely associated with the electrolyte decomposition and concomitant solid electrolyte interface (SEI) formation on both the carbon additive (Super P) and Si surface, may account for some portion of the irreversible capacity.[29] The observation that the capacity seen at 0.8 V (ca. 150 mAh g^{-1}) is much smaller than the total irreversible capacity (1210 mAh g^{-1}), however, suggests that other irreversible processes or reactions are occurring. The major irreversible reaction can be identified on the differential capacity plot (Fig. 1b), where an intense peak at 0.25 V appears in the first discharging, which is absent from the second cycle. Clearly, the major irreversible reaction, whatever it is, takes place near 0.25 V. Another revealing feature in Fig. 1b is that the peaks appeared in both first and second cycles (0.23 and 0.08 V on discharging and 0.28 and 0.45 V on charging as indicated by arrows), thus assignable as a reversible reaction, are similar in both shape and position to those of amorphous Si electrode.[30,31]

Table I. Chemical shift of ^{29}Si nuclei in some lithium silicate materials.[a]

Composition	Anionic silica	Compound	Q state	Chemical shift/ppm[a]
SiO_2	SiO_2^0	SiO_2	Q^4	−108 ± 2
Li_2O/SiO_2 = 1:2	$Si_2O_5^{2-}$	$Li_2Si_2O_5$	$2Q^3$	−92 ± 2
Li_2O/SiO_2 = 1:1	SiO_3^{2-}	Li_2SiO_3	Q^2	−75 ± 2
Li_2O/SiO_2 = 3:2	$Si_2O_7^{6-}$	$Li_6Si_2O_7$	$2Q^1$	−70 ± 2
Li_2O/SiO_2 = 2:1	SiO_4^{4-}	Li_4SiO_4	Q^0	−65 ± 2

[a] From Ref. 32-35

A detailed study on the nature of irreversible/reversible reactions and their products has been made with solid-state ^{29}Si- and ^{7}Li-NMR techniques. Table I provides the representative lithium silicate compounds (Li_2O–SiO_2) and their ^{29}Si chemical-shift data.[32-35] Here, the structural type of lithium silicates is expressed as Q^n, where the n value indicates the number of bridging Si–O–Si oxygen atoms as the silicate tetrahedral.[36] For instance, the n value of silica (SiO_2) is four as the tetrahedral units are three-dimensionally connected through four oxygen atoms, whereas n = 0 for Li_4SiO_4 because the SiO_4 tetrahedron is not connected to any neighboring ones but to four Li^+ ions. One systematic trend in the chemical shift of ^{29}Si (the last column in Table I) is the steady movement to the positive direction with a decrease in the n value, which is in good agreement with those predicted by the group electronegativity calculation made on lithium silicates.[37]

The ^{29}Si-NMR spectra for some representative silicon compounds are provided in Fig. 2a. The pure Si gives a resonance signal at −82.3 ppm, while no signal was detected for the lithiated Si ($Li_{3.5}Si$). The reason for this is not clear at present but might be due to either a peak broadening or peak shift to the outside of the common ^{29}Si chemical shift range.[38] The chemical shift of SiO_2 (−108.6 ppm) and Li_4SiO_4 (−65.0 ppm) is in good agreement with the reported values (Table I).[33] The small peak at −76.5 ppm (Q^2 state) in the latter sample comes from Li_2SiO_3 impurity. The most important observation in Fig. 2a is that SiO shows two broad bands whose chemical shifts are close to those of Si and SiO_2, which favors the RM model.

The ^{29}Si-NMR spectra were taken after the SiO electrode was cycled according to the scheme in Fig. 2b. When the electrode was discharged from 2.0 to 0.2 V and left at 0.2 V for 5 h to complete the irreversible reactions at 0.25 V, a broad peak was observed at −60 to −80 ppm at the expense of the peak located at −110.6 ppm (0.2 V trace in Fig. 2c). This illustrates that the SiO_2 component (−110.6 ppm) in SiO takes up Li^+ to produce some Si-containing compounds (−60 to −80 ppm) at 0.25 V. The most probable Si-containing compound seems to be Li_4SiO_4 as the new peak is located at −67.6 ppm (Q^0 state), but the formation of other compounds (Li_2SiO_3 or $Li_6Si_2O_7$) cannot be totally discarded because the chemical shift of these compounds also lies within the range.

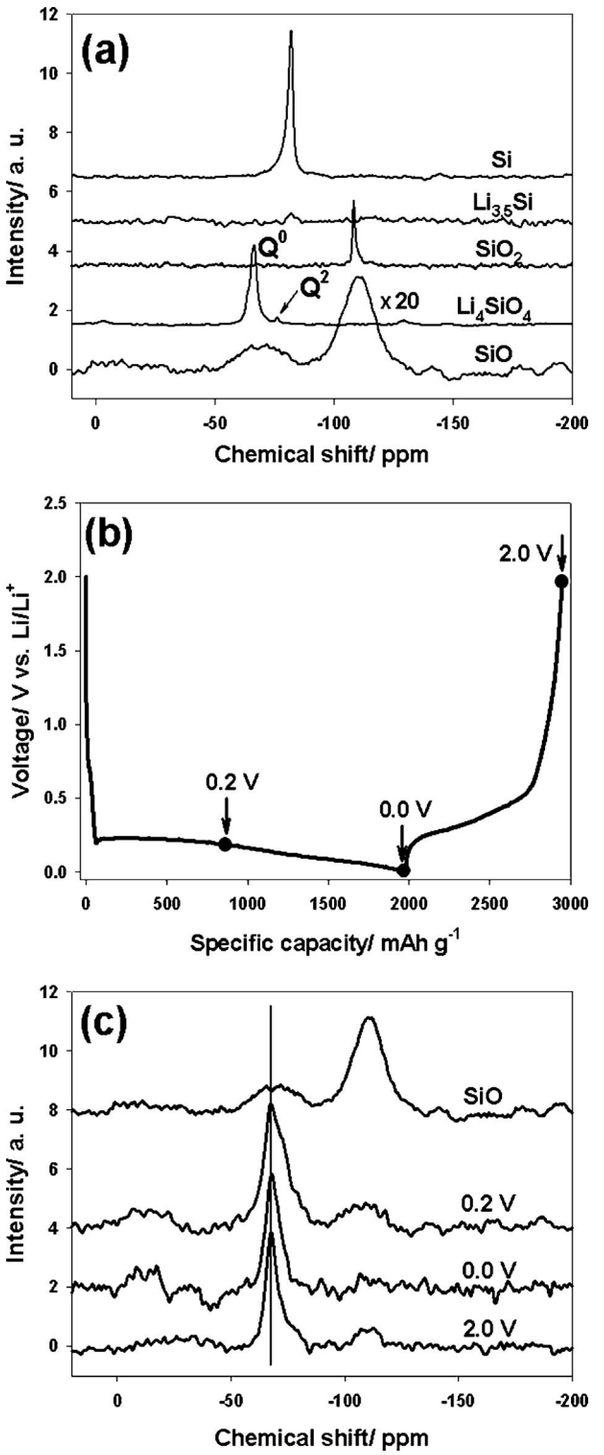

Figure 2. (a) The ^{29}Si-NMR spectra for some representative silicon-containing materials, (b) the discharge-charge voltage profile and the voltage where the NMR experiments were performed, and (c) the ^{29}Si-NMR spectra of SiO electrode recorded according to the scheme shown in (b). Note that the spectrum of SiO was multiplied by 20 times in (a).

This observation leads to a tentative conclusion that the SiO_2 domain reacts to produce lithium silicates near 0.25 V. A similar spectrum was obtained after discharging down to 0.0 V and charging up to 2.0 V. The weak or negligible SiO_2 peak at −110.6 ppm in the latter spectrum (2.0 V trace) strongly suggests that the reverse reaction from lithium silicates to SiO_2 does not occur in the charging period, that is, the lithiation of SiO_2 to lithium silicates is an irreversible reaction. The reactions associated with the Si domain in SiO cannot be clearly identified because the resonance of Si is overlapped with that of lithium silicates (Fig. 2c). This problem has been solved by using the ^{7}Li-NMR technique. The ^{7}Li-NMR spectra taken with the same cycling scheme shown in Fig. 2b are displayed in Fig. 3.

The ^{7}Li-NMR spectrum taken after discharging the SiO electrode down to 0.2 V has been deconvoluted with three Lorentzian peaks as shown in Fig. 3a. The most intense peak at 3.18 ppm can be assigned to Li_2O according to previous reports.[39-41] The peak located at 1.02 ppm is most likely due to Li_4SiO_4 because the separately synthesized Li_4SiO_4 sample gives the peak at almost the same position (1.2 ppm in the inset in Fig. 3a). The sharp peak at −1.02 ppm is believed to come from Li^+ ions either in lithium salt or SEI film.[42,43] This result suggests a formation of lithium silicate and Li_2O near 0.25 V in the first discharging period. Note that this ^{7}Li-NMR study reveals the formation of Li_2O in addition to lithium silicates, whose generation has been confirmed in the above ^{29}Si-NMR study. When the SiO electrode is discharged deeper down to 0.0 V, a new peak at 7.64 ppm develops along with the already-present three peaks responsible to lithium oxide (3.21 ppm), lithium silicate (1.20 ppm), and lithium salts (−1.0 ppm), respectively (Fig. 3b). The new peak at 7.64 ppm can be assigned to lithiated Si on the basis of the previous literature, whereby the chemical shift of ^{7}Li nuclei in Li_xSi has been reported to be ca. 10 ppm.[44] Note that the lithiation of Si domain at 0.25–0.0 V in the first discharging was already clear in the differential capacity plot (Fig. 1b). The ^{7}Li-NMR spectrum taken after charging up to 2.0 V is shown in Fig. 3c. A better fitting was obtained with one Lorentzian line (1.16 ppm) than with two or three, indicating that only lithium silicates are present after a full charging. The absence of lithiated Si (7.64 ppm) is natural because the electrode is fully charged, but the disappearance of Li_2O (3.21 ppm) after charging, which was present in the discharged electrodes (Fig. 3a and b), is unexpected. As a plausible explanation, the reaction between Li_2O and elemental Si($2Li_2O + Si \rightarrow SiO_2 + 4Li^+ + 4e$) is proposed, where the elemental Si, generated from Li_xSi by Li^+ extraction, is assumed to further react with Li_2O. As a matter of fact, there are plenty of examples demonstrating that electrochemically driven nanosized Li_2O reacts with metal nanoparticles.[21-25] This can be validated if a recovery of SiO_2 after charge is verified in the ^{29}Si-NMR spectrum, but the spectrum in Fig. 2c (2.0 V trace) does not give a solid answer due to a low signal/noise ratio.

The nature of irreversible/reversible reactions and their products that was studied by NMR technique is further ascertained from the electrode swelling/contraction profiles traced with Li^+ uptake/extraction. Figure 4 shows the electrochemical dilatometry data, where the change of electrode height was traced in the initial three cycles. An immediately apparent feature in Fig. 4a is the two-step electrode swelling in the first discharging. That is, when the electrode potential moves from 2.0 to 0.0 V, there appears a moderate electrode swelling near 0.25 V (region A), which is followed by a rather significant swelling from 0.25 to 0.0 V (region B). The former type of swelling is, however, absent in the second and third charging (Fig. 4b), strongly indicating that it is related with irreversible reactions. The later stage swelling observed at region B, however, appears in every cycle along with the contraction in the charging period, reflecting that this is associated with lithiation and delithiation of Si component in SiO because this reaction is a continuous process in nature and the volume of lithiated Si is proportional to the extent of lithiation.[45]The linear volume change of Si electrodes has also been observed in the atomic force microscopy (AFM) and electrochemical dilatometry study.[45,46] The generation of lithium silicate and lithium oxide at 0.25 V in the first discharging, which was evidenced in the NMR study (Fig. 2 and 3) and appeared as the mod-

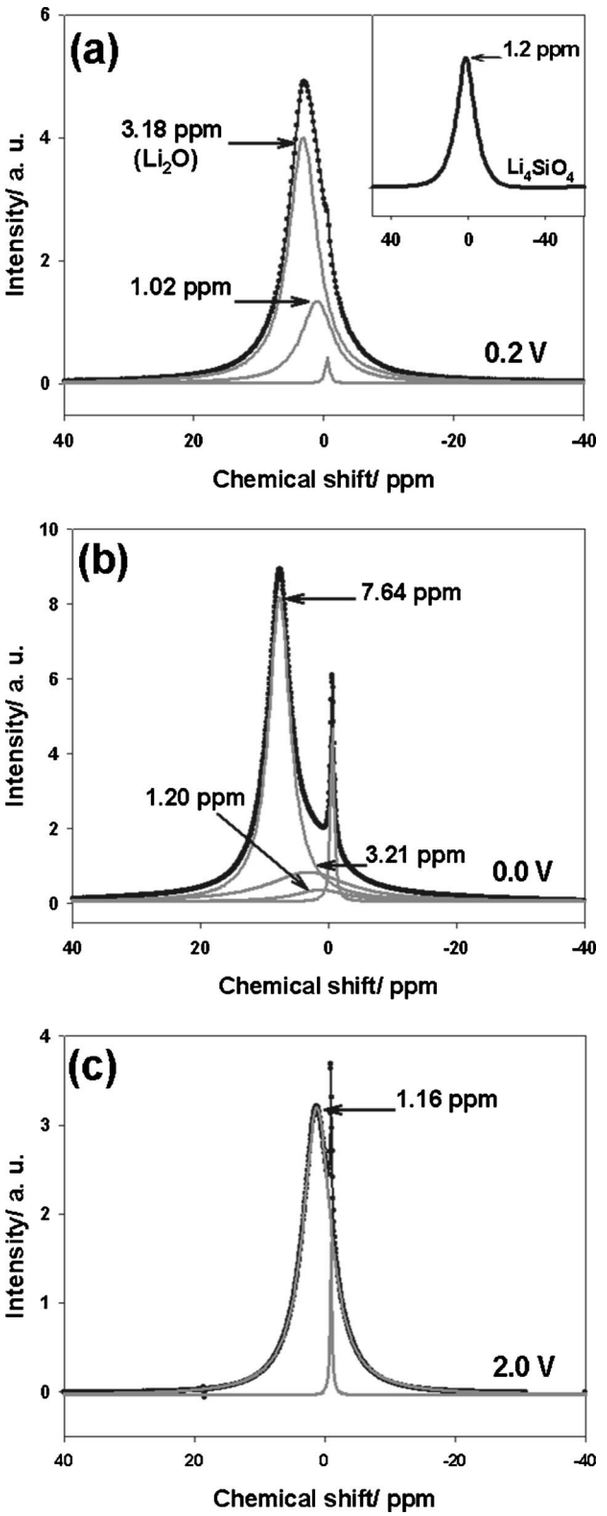

Figure 3. The ^{7}Li-NMR spectra taken with SiO electrode (a) after discharging down to 0.2 and (b) 0.0 V and (c) after charging up to 2.0 V. The spectrum of Li_4SiO_4 is provided in the inset of (a).

erate swelling in the dilatometry data, can be rationalized by the density of Li_4SiO_4 and Li_2O (Table II). Note that these oxides are denser materials than lithiated Si($Li_{3.75}Si$), implying that the formation of these oxides should lead to a less significant volume expansion than that resulted from Si lithiation.

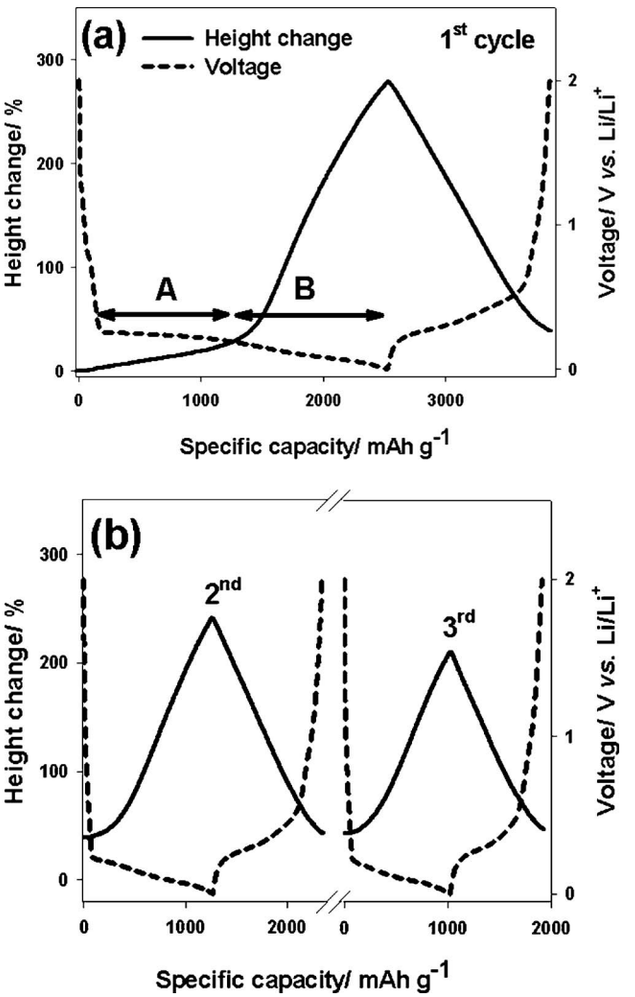

Figure 4. The electrode height change of SiO electrode traced by electrochemical dilatometer: (a) first cycle and (b) second and third cycle. Note the two-step electrode swelling in the first cycle.

A combined study of NMR, dilatometry, and charge-discharge cycling consistently demonstrates that SiO is composed of two separate domains, elemental Si and SiO_2. The SiO_2 domain is irreversibly lithiated in the first discharging to produce lithium oxide and lithium silicate, whereas the Si domain reversibly reacts with Li^+ and electrons. Here, two points would be of value to be addressed. First, SiO_2 is known to be inactive with Li^+, but its reactivity is clearly demonstrated in this work. Additional evidence for the reactivity of SiO_2 can be found in Fig. 1a, where the first discharging capacity amounts to 2680 mAh g^{-1}. If only the Si domain is assumed to be active while the SiO_2 being inactive, the discharging

Table II. Density of some Li- and Si-containing materials.

Material	Density (g cm^{-3})
Si	2.33
SiO	2.18[a]
SiO_2 (Quartz)	2.65
Li_4SiO_4	2.39
Li_2O	2.02
$Li_{3.75}Si$	1.18[a]

[a] Calculated from the data provided by Ref. 30

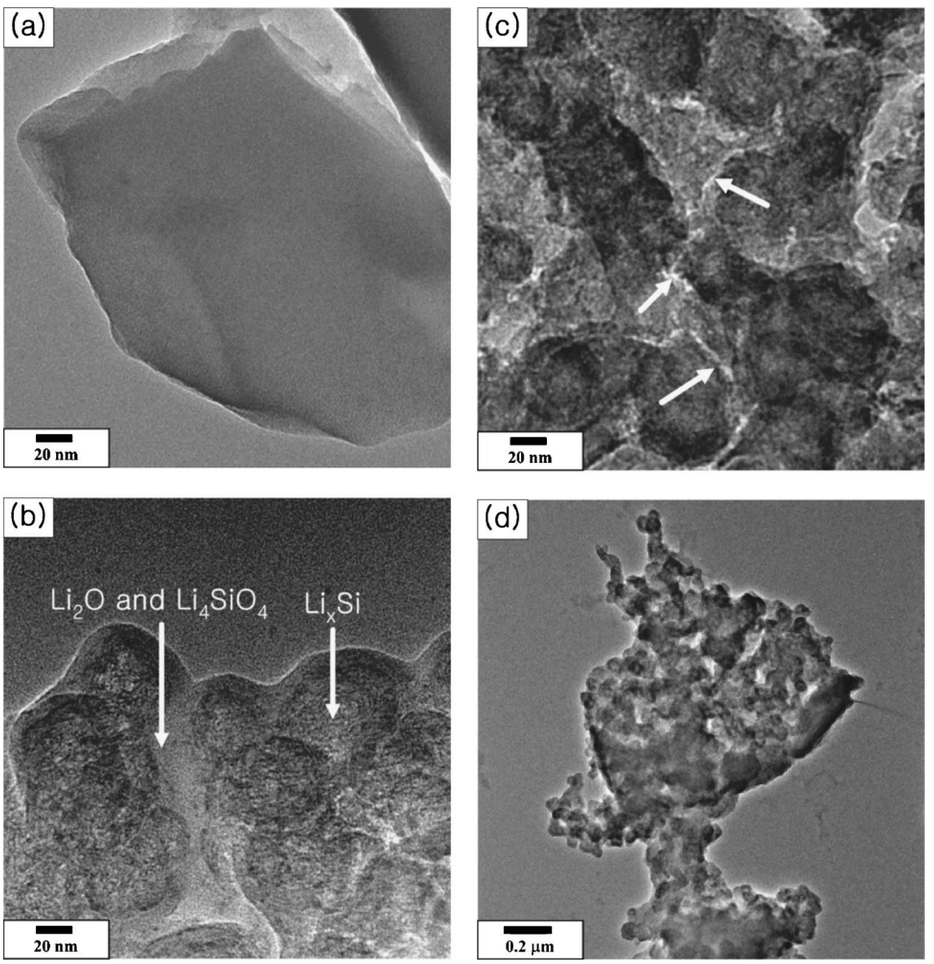

Figure 5. The TEM images of SiO particles taken (a) before cycling, (b) after first discharging, (c) after first charging, and (d) after 20 cycles.

capacity of SiO is calculated to be 1142 mAh g^{-1}. This cannot account for the observed value (2680 mAh g^{-1}), even if the irreversible capacity associated with SEI formation (ca. 150 mAh g^{-1}) and capacitive charging capacity ($<$150 mAh g^{-1}) that was estimated from the initial sloping region in the charging profile in Fig. 1a are considered.[23] Rather, the observed first discharging capacity should be explained by Li^+ uptake by the SiO_2 in addition to Si domain. The reactivity of SiO_2 domain may be explained by its extremely small size (less than 10 Å) as many reports claim a reactivity of nanosized electrode materials, which cannot be found with bulkier materials.[21-26] Another interesting feature observed in this work is that the Si domain, which is present as an amorphous state in the initial stage, remains amorphous even if it is discharged down to 0.0 V. It is somewhat contrary to the previous observation, whereby amorphous Si recrystallizes at 0.05 V in the discharging period to form $Li_{15}Si_4$ phase.[30] The absence of recrystallization is a desirable feature because it is known to cause an inhomogeneous volume expansion and crack formation within the Si matrix.

In order to see what effects the lithium silicate/lithium oxide formation has on the anodic performance of SiO, the postmortem analysis was made on the cycled electrodes. The TEM image of initial SiO is shown in Fig. 5a. Even if the SiO is supposed to be a mixture of Si and SiO_2 domain, the image looks like a single phase because of the small domain size. The TEM image taken after a full discharging exhibits a totally different morphology as shown in Fig. 5b. The wrinkled dumbbell-like particles and a lighter image at the interfacial sites can be located. Because the dumbbell-like morphology is characteristic to lithiated silicon,[47] the lighter image can be assigned to Li_2O and lithium silicates. It is, however, seen that the initially nanosized Si domain has been grown to be aggregated bigger particles (5–60 nm); even further, they are segregated from the lithium silicates/Li_2O phase. This reflects the instability of nanosized materials having a large interface area.[48] The size of lithiated Si particles, however, decreases upon charging, accompanied by a crack formation at the interface (indicated by arrows), which must be resulted from a volume contraction in the Si particles. The TEM image of SiO electrode taken after 20 cycles is shown in Fig. 5d, where a pulverization resulted from a severe phase segregation is noticed. It is likely that the lithium silicates/Li_2O phase plays a buffering action against the volume change of Si domains because they are located between the Si particles.[19] In the situation where the pulverization is severe, however, it is questionable if the buffering role is indeed prevailing. The steady capacity fading shown in Fig. 1a may be the result of this pulverization.

Conclusion

In this work, the microstructure and electrochemical performance of SiO were investigated using solid-state NMR and electrochemical dilatometry technique. The following points are summarized.

1. The ^{29}Si MAS-NMR spectra of SiO show two different resonances whose chemical shift values are close to those of elemental-state Si and SiO_2, suggesting that the RM model is the more appropriate description for SiO microstructure.

2. Contrary to the micrometer-sized SiO_2, the nanosized SiO_2 domain in SiO reacts with lithium. This must be one of the examples that nanosized alloys and metal oxides show unexpected electrochemical reactivity.

3. The electrochemical dilatometry was successfully utilized for

the study of electrode swelling/contraction. In this particular study, the irreversible formation of lithium silicates and lithium oxide and reversible lithiation/de-lithiation of Si domain were ascertained from the difference in electrode swelling between two processes.

4. It was found that two nanosized domains in SiO were aggregated by themselves to be separate lithium silicates/lithium oxide and lithiated Si phase after cycling. This reflects the instability of nanosized amorphous mixture having a larger interface area. In this work, the crack formation at the two-phase boundaries and pulverization were observed, which should be minimized by any modification or optimization of SiO electrodes.

Acknowledgments

This work was supported by KOSEF via the Research Center for Energy Conversion and Storage. We are grateful to the Daegu Center at the Korea Basic Science Institute for helpful discussions and NMR measurements. We also acknowledge Dr. R. Kötz and Dr. P. Novak (Paul Scherrer Institute, Switzerland) for their assistance in fabricating the electrochemical dilatometer.

Seoul National University assisted in meeting the publication costs of this article.

References

1. C. J. Wen and R. A. Huggins, *J. Solid State Chem.*, **37**, 271 (1976).
2. J. O. Besenhard, J. Yang, and M. Winter, *J. Power Sources*, **68**, 87 (1997).
3. M. Yoshio, H. Wang, K. Fukuda, T. Umeno, N. Dimov, and Z. Ogumi, *J. Electrochem. Soc.*, **149**, A1598 (2002).
4. A. M. Wilson and J. R. Dahn, *J. Electrochem. Soc.*, **142**, 326 (1995).
5. H. Li, X. Huang, L. Chen, Z. Wu, and Y. Liang, *Electrochem. Solid-State Lett.*, **2**, 547 (1999).
6. I. S. Kim, P. N. Kumta, and G. E. Blomgren, *Electrochem. Solid-State Lett.*, **3**, A493 (2000).
7. H. Y. Lee and S. M. Lee, *J. Power Sources*, **112**, 649 (2002).
8. I. S. Kim, G. E. Blomgren, and P. N. Kumta, *Electrochem. Solid-State Lett.*, **6**, A157 (2003).
9. Y. Liu, T. Matsumura, N. Imanishi, A. Hirano, T. Ichikawa, and Y. Takeda, *Electrochem. Solid-State Lett.*, **8**, A599 (2005).
10. Z. P. Guo, E. Milin, J. Z. Wang, J. Chen, and H. K. Liu, *J. Electrochem. Soc.*, **152**, A2211 (2005).
11. J. Yang, Y. Takeda, N. Imanishi, C. Capiflia, J. Y. Xie, and O. Yamanoto, *Solid State Ionics*, **152**, 125 (2002).
12. Y. Liu, K. Hanai, J. Yang, N. Imanishi, A. Hirano, Y. Hirano, and Y. Takeda, *Solid State Ionics*, **168**, 61 (2004).
13. Y. Nagao, H. Sakaguchi, H. Honda, T. Fukunaga, and T. Esaka, *J. Electrochem. Soc.*, **151**, A1572 (2004).
14. Y. Liu, J. Yang, N. Imanishi, A. Hirano, Y. Takeda, and O. Yamamoto, *J. Power Sources*, **146**, 376 (2005).
15. H. R. Phillip, *J. Phys. Chem. Solids*, **32**, 1935 (1971).
16. R. J. Temkin, *J. Non-Cryst. Solids*, **17**, 215 (1975).
17. B. Friede and M. Jansen, *J. Non-Cryst. Solids*, **204**, 202 (1996).
18. A. Hohl, T. Wider, P. A. Aken, T. E. Weirich, G. Denninger, M. Vidal, S. Oswald, C. Deneke, J. Mayer, and H. Fuess, *J. Non-Cryst. Solids*, **320**, 255 (2003).
19. M. Miyachi, H. Yamamoto, H. Kawai, T. Ohta, and M. Shirakata, *J. Electrochem. Soc.*, **152**, A2089 (2005).
20. X. Yang, Z. Wen, X. Xu, B. Lin, and S. Huang, *J. Power Sources*, **164**, 880 (2007).
21. J. Jamnik and J. Maier, *Phys. Chem. Chem. Phys.*, **5**, 5215 (2003)
22. P. Poizot, S. Laruelle, S. Grugeon, L. Dupont, and J. M. Tarascon, *Nature (London)*, **407**, 496 (2000).
23. P. Balaya, H. Li, L. Kienle, and J. Maier, *Adv. Funct. Mater.*, **13**, 621 (2003).
24. H. Li, P. Balaya, and J. Maier, *J. Electrochem. Soc.*, **151**, A1878 (2004).
25. H. Li, G. Richter, and J. Maier, *Adv. Mater. (Weinheim, Ger.)*, **15**, 736 (2003).
26. F. Badway, N. Pereira, F. Cosandey, and G. G. Amatucci, *J. Electrochem. Soc.*, **150**, A1209 (2003).
27. M. Winter, G. H. Wrodnig, J. O. Besenhard, W. Biberacher, and P. Novak, *J. Electrochem. Soc.*, **147**, 2427 (2000).
28. M. Hahn, O. Barbieri, F. P. Campana, R. Kötz, and R. Gallay, *Appl. Phys. A*, **82**, 633 (2006).
29. A. S. Claye, J. E. Fischer, C. B. Huffman, A. G. Rinzler, and R. E. Smalley, *J. Electrochem. Soc.*, **147**, 2845 (2000).
30. M. N. Obrovac and L. Christensen, *Electrochem. Solid-State Lett.*, **7**, A93 (2004).
31. J. H. Ryu, J. W. Kim, Y. E. Sung, and S. M. Oh, *Electrochem. Solid-State Lett.*, **7**, A306 (2004).
32. H. Maekawa, T. Maekawa, K. Katsuyuki, and T. Yokokawa, *J. Non-Cryst. Solids*, **127**, 53 (1991).
33. M. Takahashi, H. Toyuki, M. Tatsunisago, and T. Minamai, *Solid State Ionics*, **86-88**, 535 (1996).
34. N. J. Clayden, S. Esposito, U. A. Jayasooriya, J. Sprunt, and P. Pernice, *J. Non-Cryst. Solids*, **224**, 50 (1998).
35. T. Fuss, A. M. Milankovic, C. S. Ray, C. E. Lesher, R. Youngman, and D. E. Day, *J. Non-Cryst. Solids*, **352**, 4101 (2006).
36. J. Deubener, *J. Non-Cryst. Solids*, **351**, 1500 (2005).
37. N. Janes and E. Oldfield, *J. Am. Chem. Soc.*, **107**, 6769 (1985).
38. W. L. Shao, J. Shinar, and B. C. Gerstein, *Phys. Rev. B*, **41**, 9491 (1990).
39. G. R. Goward, F. Leroux, W. P. Power, G. Ouvrard, W. Dmowski, T. Egami, and L. F. Nazar, *Electrochem. Solid-State Lett.*, **2**, 367 (1999).
40. G. R. Goward, L. F. Nazar, and W. P. Power, *J. Mater. Chem.*, **10**, 1241 (2000).
41. B. M. Mayer, N. Leifer, S. Sakamoto, S. G. Greenbaum, and C. P. Grey, *Electrochem. Solid-State Lett.*, **8**, A147 (2005).
42. M. Letellier, F. Chevallier, F. Beguin, E. Frackowiak, and J. N. Rouzaud, *J. Phys. Chem. Solids*, **65**, 245 (2004).
43. M. Letellier, F. Chevallier, and F. Beguin, *J. Phys. Chem. Solids*, **67**, 1228 (2006).
44. L. A. Stearns, J. Gryko, J. Diefenbacher, G. K. Ramachandran, and P. F. McMillan, *J. Solid State Chem.*, **173**, 251 (2003).
45. M. Holzapfel, H. Buqa, L. J. Hardwick, M. Hahn, A. Wursig, W. Scheifele, P. Novak, R. Kötz, C. Veit, and F. M. Petrat, *Electrochim. Acta*, **52**, 973 (2006).
46. L. Y. Beaulieu, T. D. Hatchard, A. Bonakdarpour, M. D. Fleischauer, and J. R. Dahn, *J. Electrochem. Soc.*, **150**, A1457 (2003).
47. T. Kim, S. Park, and S. M. Oh, *Electrochem. Commun.*, **8**, 1461 (2006).
48. G. Wilde, *Surf. Interface Anal.*, **38**, 1047 (2006).